Eur. Phys. J. B **54**, 457–464 (2006)
DOI: 10.1140/epjb/e2007-00028-4

THE EUROPEAN PHYSICAL JOURNAL B

The short-range correlations of a doped Mott insulator

T.C. Ribeiro[a]

Department of Physics, University of California, Berkeley, California 94720, USA
and
Material Sciences Division, Lawrence Berkeley National Laboratory, Berkeley, California 94720, USA

Received 24 September 2006 / Received in final form 23 December 2006
Published online 3 February 2007 –

Abstract. This paper presents numerical studies of the single hole $tt't''J$ model that address the interplay between the kinetic energy of itinerant electrons and the exchange energy of local moments as of interest to doped Mott insulators. Due to this interplay, two different spin correlations coexist around a mobile vacancy. These *local* correlations provide an effective two-band picture that explains the two-band structure observed in various theoretical and experimental studies, the doping dependence of the momentum space anisotropic pseudogap phenomena and the asymmetry between hole and electron doped cuprates.

PACS. 71.10.Fd Lattice fermion models – 74.25.Jb Electronic structure – 74.72.-h Cuprate superconductors

1 Introduction

The evolution between the weakly correlated Fermi metal and the strongly coupled Mott insulator is a major and long-standing problem in the field of condensed matter physics [1–3]. It concerns a vast list of material compounds [4] where the local character of d and f orbitals enhances the electron effective mass together with the role of the electron-electron Coulomb repulsive interaction. The resulting competition between the small kinetic energy and the strong interaction may lead itinerant electrons in the metallic state to form local moments in the Mott insulating state [1]. In this paper, I focus on the interplay between such itinerant and localized electrons.

The generalized-tJ model explicitly embodies the above interplay. Indeed, "t" stands for the kinetic energy term of itinerant charge carriers and "J" stands for the interaction term between localized spins. The intricacy of this model follows from the mutual frustration between these two terms. Specifically, the $J > 0$ term favors a staggered moment spin background that constrains the motion of vacancies, while the t term moves electrons around and, thus, reshuffles and destroys the underlying antiferromagnetic (AF) spin pattern. The two-dimensional (2D) $tt't''J$ model, which this paper addresses, is especially interesting because the compromise between the spin exchange and hole kinetic energies is particularly subtle in the parameter regime of interest to real materials, such as the high-temperature superconducting cuprates [5–7].

Following the recent improvement in computational resources, experimental resolution and sample quality, various non-trivial results have illuminated our understanding of 2D doped Mott insulators. It is exciting to note that many of these results are consistently obtained by different theoretical approaches and by experiments. For instance, a variety of numerical and analytical studies show that the electronic spectrum below the chemical potential has a robust two-band structure and that changing the electron density redistributes the spectral weight in a momentum dependent way [8–17]. Similar conclusions apply to the two dispersive features displayed by angle-resolved photoemission spectroscopy (ARPES) on the cuprates [18–22]. Since the electron dynamics in strongly correlated systems follows from the local environment around the carriers [23], the above two-band structure reflects the presence of two local correlations, which arise due to the interplay between itinerant electrons and local moments.

This paper explores the microscopic origin of the above short-range correlations and, thus, of the aforementioned two-band structure that appears in both theory and experiments. Specifically, in Section 2 the exact diagonalization and the self-consistent Born approximation techniques are employed to study the single hole problem in the $tt't''J$ model. I show that the interplay between the "t" and "J" terms of the Hamiltonian translates into the coexistence of two different types of spin correlations around the vacancy — one type is driven by the kinetic energy term and the other by the exchange energy term. These short-range correlations, which follow from purely local energetic considerations and whose properties are studied in Section 3, underlie a diverse set of non-trivial and, by now,

[a] *Current address:* Global Modelling and Analytics Group, Credit Suisse, One Cabot Square, London, E14 4QJ, UK
e-mail: tribeiro@mit.edu

well established properties of 2D doped Mott insulators. These include the doping dependence of the pseudogap dispersion and of the pseudogap momentum space spectral weight distribution [18,19,21,24–27], as well as the asymmetry between the hole and electron doped regimes of the cuprate compounds (Sect. 4) [9,10,14,18,19,21,25,28,29].

2 Two local correlations

2.1 The model system

The single hole 2D $tt't''J$ Hamiltonian is

$$H_{tt't''J} = -\sum_{\langle ij\rangle,\sigma} t_{ij}\left(\widetilde{c}^{\dagger}_{i,\sigma}\widetilde{c}_{j,\sigma} + H.c.\right) + \sum_{\langle ij\rangle} J_{ij}\boldsymbol{S}_i.\boldsymbol{S}_j \quad (1)$$

where $\widetilde{c}_{i,\sigma} = c_{i,\sigma}(1 - n_{i,-\sigma})$ is the constrained electron operator. t_{ij} equals t, t' and t'' for first, second and third nearest-neighbor (NN) sites respectively and vanishes otherwise. The exchange interaction only involves NN spins for which $J_{ij} = J$. In this paper $J \in [0.2, 0.8]$ (units are set so that $t = 1$), which includes the experimentally relevant regime $J \approx 0.4$. The calculations are not extended down to $J = 0$ because, in that limit, the hole is subjected to the Nagaoka instability [30] and, thus, the physics for $J \approx 0$ is specific to such a regime and is not relevant to materials like the cuprates [31]. The calculations for $J > 0.8$ do not change the argument below nor the consequent conclusions.

As mentioned in Section 1, this paper addresses the electron dynamics as probed by the electron spectral function. Its focus does not lie in the full details of the spectral function line shape, but rather on the fact that the electronic spectrum displays two separate dispersive features below the Fermi level. This work also concerns the momentum distribution of electron spectral weight, which displays distinct behavior in separate regions of the Brillouin zone, namely the regions around $(\pi/2, \pi/2)$ and $(\pi, 0)$. The above facts encode short time and short length scale physics. Hence, within the above context, it is relevant to study small lattice systems and, unless otherwise stated, all the results below come from the exact diagonalization of $H_{tt't''J}$ on a 4×4 lattice. The exact diagonalization analysis is further substantiated by results from the self-consistent Born approximation approach to the spinless-fermion Schwinger-boson representation of the tJ model [32–34] on a 16×16 lattice.

2.2 One-hole states

There exist two extreme limits where the interplay between itinerant electrons and local moments occurs, namely the one where: (i) most electrons are itinerant and the corresponding Fermi energy is the highest energy scale in the problem; (ii) most electrons form local moments and the system reduces to a lattice of spins with a few mobile vacancies. The former case is captured by the well understood Kondo model, which addresses how the Fermi sea accommodates the presence of a local moment [35]. The second case, which is of interest close to the Mott insulator transition, differs from the standard Kondo lattice problem since the spin-spin interaction is larger than the itinerant electrons' Fermi energy [36]. In this case, it is rather convenient to consider how the spin background adjusts to the presence of a hole.

Hence, in what follows, one studies the lowest energy configurations of the spin background around a single vacancy. In particular, one considers the lowest energy single hole state $|\psi_{\boldsymbol{k}}, J, t't,''\rangle$ for each momentum $\boldsymbol{k}$, where J, t' and t'' label the model parameters that define the corresponding Hamiltonian $H_{tt't''J}$. This state can fall into two categories — it either has zero or non-zero quasiparticle spectral weight $|\langle\psi_{\boldsymbol{k}}, J, t', t''|\widetilde{c}_{\boldsymbol{k},\sigma}|\text{HF GS}\rangle|^2$, where $|\text{HF GS}\rangle$ denotes the groundstate of the half-filled system. For all $\boldsymbol{k}$, t' and t'' there exists a certain $J_c(\boldsymbol{k}, t', t'')$ such that $|\psi_{\boldsymbol{k}}, J, t', t''\rangle$ has zero quasiparticle spectral weight if and only if $J \leq J_c(\boldsymbol{k}, t', t'')$. The intuition behind this result is that for $J/t \gg 1$ the large spin stiffness renders the spin background robust to hole motion, while for small enough J/t the soft AF spin configuration is dramatically modified by the doped hole (the Nagaoka instability [30] perfectly illustrates this last case). If $J \leq J_c(\boldsymbol{k}, t', t'')$ one denotes $|\psi_{\boldsymbol{k}}, J, t't,''\rangle$ by $|\widetilde{U}_{\boldsymbol{k}}, J, t', t''\rangle$ (hence, by definition, $|\widetilde{U}_{\boldsymbol{k}}, J, t', t''\rangle$ has vanishing quasiparticle spectral weight). If, instead, $J > J_c(\boldsymbol{k}, t', t'')$ the single hole state $|\psi_{\boldsymbol{k}}, J, t't,''\rangle$ can be approximately recast as

$$|\psi_{\boldsymbol{k}}, J, t', t''\rangle \cong\ q(\boldsymbol{k}, J, t', t'')|Q_{\boldsymbol{k}}, t', t''\rangle + u(\boldsymbol{k}, J, t', t'')|U_{\boldsymbol{k}}, t', t''\rangle \quad (2)$$

where $|Q_{\boldsymbol{k}}, t', t''\rangle$ and $|U_{\boldsymbol{k}}, t', t''\rangle$ are orthonormal states (to be defined below) that do *not* depend on J [37],

while $q(\boldsymbol{k}, J, t', t'')$ and $u(\boldsymbol{k}, J, t', t'')$ are J-dependent coefficients that obey the normalization condition $|q(\boldsymbol{k}, J, t', t'')|^2 + |u(\boldsymbol{k}, J, t', t'')|^2 = 1$. Equation (2), which applies in a large range of J values, is a major result in this paper. It implies that, in a large interval of values of $J > J_c(\boldsymbol{k}, t', t'')$, the eigenstates $|\psi_{\boldsymbol{k}}, J, t't,''\rangle$ define a line parameterized by J which approximately lies in a 2D plane in the single hole $tt't''J$ model Hilbert space. The physical content of this statement, together with evidence supporting equation (2), are presented below.

If $t', t'' = 0$ then $J_c(\boldsymbol{k}, t' = 0, t'' = 0) < 0.2$ for all $\boldsymbol{k}$ in Table 1. This table shows that for all $J \in [0.2, 0.8]$, as well as for all depicted momenta $\boldsymbol{k}$, the states $|\psi_{\boldsymbol{k}}, J, t' = 0, t'' = 0\rangle$ have almost unit overlap with the 2D Hilbert space $\{|\psi_{\boldsymbol{k}}, J = 0.2, t = 0', t'' = 0\rangle, |\psi_{\boldsymbol{k}}, J = 0.6, t' = 0, t'' = 0\rangle\}$. This conclusion is further substantiated by the self-consistent Born approximation technique on a 16×16 lattice (see Tab. 1), thus showing that the above result is not specific to the 4×4 lattice used in the exact diagonalization calculation [38]. A very similar observation holds when $t', t'' \neq 0$, as Table 1 illustrates for $t' = -0.2$, $t'' = 0.1$. The only difference between the above $t', t'' = 0$ and $t' = -0.2$, $t'' = 0.1$ cases is that $J_c(\boldsymbol{k} = (\pi, 0), t' = 0, t'' = 0) < 0.2$ while $0.3 < J_c(\boldsymbol{k} = (\pi, 0), t' = -0.2, t'' = 0.1) < 0.4$. Since the approximate equality in equation (2) only applies for

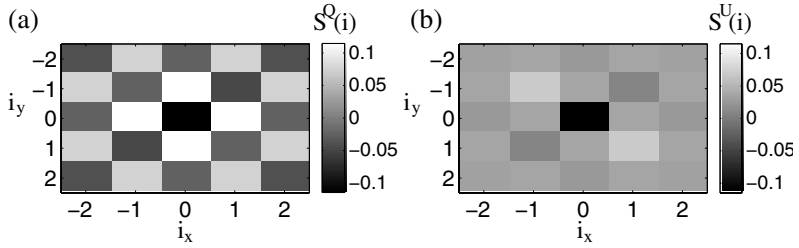

Fig. 1. (a) $S^Q_{\boldsymbol{k}}(\boldsymbol{i})$ and (b) $S^U_{\boldsymbol{k}}(\boldsymbol{i})$ where $\boldsymbol{i}$ is the distance to the vacancy (black square at the center), $\boldsymbol{k} = (\pi/2, \pi/2)$ and $t', t'' = 0$. Different $\boldsymbol{k}$, t' and t'' lead to qualitatively similar conclusions, as seen in Figure 2.

Table 1. Square of the overlap of $|\psi_{\boldsymbol{k}}, J, t', t''\rangle$ with the Hilbert space $\{|\psi_{\boldsymbol{k}}, J = 0.2, t', t''\rangle, |\psi_{\boldsymbol{k}}, J = 0.6, t', t''\rangle\}$ for different J and $\boldsymbol{k}$. Both exact diagonalization (ED) and self-consistent Born approximation (SCBA) results are shown for $t', t'' = 0$. Exact diagonalization results are also shown for $t' = -0.2$, $t'' = 0.1$. For $t' = -0.2$, $t'' = 0.1$ and $\boldsymbol{k} = (\pi, 0)$ the Hilbert space $\{|\psi_{\boldsymbol{k}}, J = 0.4, t', t''\rangle, |\psi_{\boldsymbol{k}}, J = 0.8, t', t''\rangle\}$ is used instead.

	J	0.3	0.4	0.5	0.6	0.7	0.8
	$(\frac{\pi}{2}, \frac{\pi}{2})$	0.9994	0.9994	0.9998	1	0.9998	0.9990
$t' = 0$	$(\pi, 0)$	0.9994	0.9994	0.9998	1	0.9998	0.9990
$t'' = 0$	$(\pi, \frac{\pi}{2})$	0.9972	0.9977	0.9993	1	0.9992	0.9970
ED	$(\frac{\pi}{2}, 0)$	0.9975	0.9980	0.9994	1	0.9994	0.9977
	$(0, 0)$	0.9946	0.9923	0.9963	1	0.9938	0.9766
	$(\frac{\pi}{2}, \frac{\pi}{2})$	0.9996	0.9996	0.9998	1	0.9998	0.9990
$t' = 0$	$(\pi, 0)$	0.9994	0.9994	0.9998	1	0.9997	0.9986
$t'' = 0$	$(\pi, \frac{\pi}{2})$	0.9989	0.9988	0.9996	1	0.9995	0.9978
SCBA	$(\frac{\pi}{2}, 0)$	0.9989	0.9988	0.9996	1	0.9995	0.9978
	$(0, 0)$	0.9016	0.9005	0.9766	1	0.9842	0.9488
	$(\frac{\pi}{2}, \frac{\pi}{2})$	0.9994	0.9994	0.9998	1	0.9998	0.9990
$t' = -0.2$	$(\pi, 0)$	–	1	0.9998	0.9997	0.9999	1
$t'' = 0.1$	$(\pi, \frac{\pi}{2})$	0.9936	0.9952	0.9986	1	0.9987	0.9950
ED	$(\frac{\pi}{2}, 0)$	0.9907	0.9943	0.9986	1	0.9988	0.9957
	$(0, 0)$	0.9880	0.9856	0.9943	1	0.9940	0.9807

$J > J_c(\boldsymbol{k}, t', t'')$, in Table 1 one uses the 2D Hilbert space $\{|\psi_{\boldsymbol{k}=(\pi,0)}, J = 0.4, t' = -0.2, t'' = 0.1\rangle, |\psi_{\boldsymbol{k}=(\pi,0)}, J = 0.8, t' = -0.2, t'' = 0.1\rangle\}$ to illustrate that equation (2) also applies when $\boldsymbol{k} = (\pi, 0)$ and $t' = -0.2$, $t'' = 0.1$.

The above numerical results show that equation (2) is a very good approximation for a wide range of values of the exchange coupling J [39]. However, one is still free to choose any orthonormal pair of states $|Q_{\boldsymbol{k}}, t', t''\rangle$ and $|U_{\boldsymbol{k}}, t', t''\rangle$ in the 2D Hilbert space used as reference. A physically sensible choice comes from requiring $q(\boldsymbol{k}, J, t', t'')$ to monotonously increase with J/t [$u(\boldsymbol{k}, J, t', t'')$ thus decreases monotonously with J/t]. Since cranking up J enhances the quasiparticle features of doped carriers [32], the above condition is automatically satisfied if $|U_{\boldsymbol{k}}, t', t''\rangle$ has vanishing quasiparticle spectral weight. This prescription uniquely determines Q states ($|Q_{\boldsymbol{k}}, t', t''\rangle$) and U states ($|U_{\boldsymbol{k}}, t', t''\rangle$) which, one should note, are not eigenstates of $H_{tt't''J}$ [40]. The above construction implies that Q states bear the electron-like properties of the true eigenstates $|\psi_{\boldsymbol{k}}, J, t't,''\rangle$ and, indeed, for all values of t' and t'' used throughout this paper $0.5 \lesssim \frac{|\langle Q_{\boldsymbol{k}}|\widetilde{c}_{\boldsymbol{k},\sigma}|\text{HF GS}\rangle|^2}{|\langle \text{HF GS}|\widetilde{c}^\dagger_{\boldsymbol{k},\sigma}\widetilde{c}_{\boldsymbol{k},\sigma}|\text{HF GS}\rangle|} \lesssim 0.8$ in the momentum space region around the $(\pi, 0) - (0, \pi)$ line [41].

The previous argument clarifies how the spin background adjusts to the presence of a moving hole. Specifically, spins show two different types of correlations — one type is enhanced upon increasing J/t and the other becomes more pronounced when J/t is reduced. By definition, Q and U states capture these correlations and, not surprisingly, they display distinct physical properties. Simply based on the above energetic considerations, one expects the former states to retain the AF correlations of the undoped system, while the doping induced spin correlations in U states facilitate hole hopping. The analysis in Section 3.1 confirms this microscopic picture. In principle, a similar construction applies to models other than the 2D $tt't''J$ model. The significant fact about this model is that, for experimentally relevant parameters, the overlap of both Q and U states with $|\psi_{\boldsymbol{k}}, J, t', t''\rangle$ is large and exhibits a considerable momentum dependence (see Sect. 4) [42].

3 Properties of the local correlations

The construction in Section 2.2 identifies two different spin configurations that coexist around a mobile vacancy. It also provides a recipe to separately obtain these configurations and, thus, to study their properties.

3.1 Real and momentum space properties

First, consider the average spin density pattern around the hole

$$S^Y_{\boldsymbol{k}}(\boldsymbol{i}) \equiv \left\langle Y_{\boldsymbol{k}} \left|_j S^z_{j+i} \widetilde{c}_{j,-1/2} \widetilde{c}_{j,-1/2}\right| |Y_{\boldsymbol{k}}\rangle \right\rangle \qquad (3)$$

for both $Y = Q$ and $Y = U$. Figure 1 illustrates how different the spin background is in Q and U states for $\boldsymbol{k} = (\pi/2, \pi/2)$ and $t', t'' = 0$. The former preserve an evident staggered pattern while the latter display an almost uniform distribution of the spin-1/2 introduced in the system upon doping. To show that this picture remains valid for other values of $\boldsymbol{k}$, t' and t'', one takes the average of the staggered magnetization over the hole's νth NN sites: $\widetilde{S}^Y_{\boldsymbol{k}}(\nu) \equiv -\langle(-)^{i_x+i_y} S^Y_{\boldsymbol{k}}(\boldsymbol{i})\rangle_\nu - \frac{1}{N-1}\frac{1}{2}$ (here $Y = Q, U$) [43]. Figures 2a, 2c and 2e show that for different $\boldsymbol{k}$, t' and t''

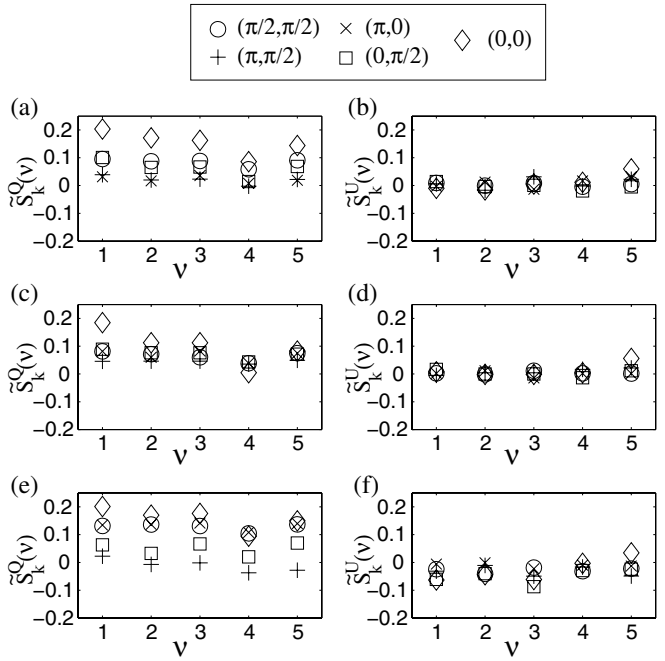

Fig. 2. $\widetilde{S}^{Q}_{\boldsymbol{k}}(\nu)$ (left panels) and $\widetilde{S}^{U}_{\boldsymbol{k}}(\nu)$ (right panels) for different momenta $\boldsymbol{k}$. (a) and (b) $t' = -0.3, t'' = 0.2$. (c) and (d) $t', t'' = 0$. (e) and (f) $t' = 0.3, t'' = -0.2$.

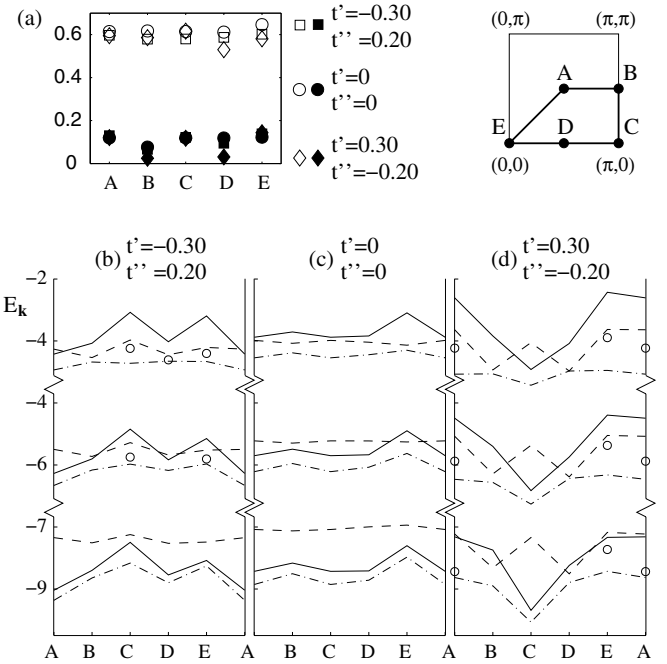

Fig. 3. (a) $\sum'_{\boldsymbol{q}} n^{U}_{\boldsymbol{k}}(\boldsymbol{q}, +1/2)$. Empty symbols involve sum over $\boldsymbol{q} = (\pi, \pi)$, $\boldsymbol{q} = (\pm\pi/2, \pi)$ and $\boldsymbol{q} = (\pi, \pm\pi/2)$. Full symbols involve sum over $\boldsymbol{q} = (0, 0)$, $\boldsymbol{q} = (\pm\pi/2, 0)$ and $\boldsymbol{q} = (0, \pm\pi/2)$. (b)–(d) Dispersion relations for $|Q_{\boldsymbol{k}}\rangle$ (full line), $|U_{\boldsymbol{k}}\rangle$ (dashed line) and $|\psi_{\boldsymbol{k}}\rangle$ (dash-dot line). Upper, middle and lower set of dispersions are obtained for J equal to 0.2, 0.4 and 0.7 respectively. (∘) Indicates the best energy obtained by a linear combination of $|Q_{\boldsymbol{k}}\rangle$ and $|U_{\boldsymbol{k}}\rangle$ when $J < J_c(\boldsymbol{k}, t', t'')$ (in which case $|\psi_{\boldsymbol{k}}\rangle = |\widetilde{U}_{\boldsymbol{k}}, J, t', t''\rangle$).

the doped hole in Q states coexists with the staggered spin pattern inherited from the undoped system. This state of affairs contrasts with the results for U states, where the AF spin pattern of the undoped system is destroyed and the staggered magnetization around the hole is close zero and even negative (Figs. 2b, 2d and 2f). One can check that a similar conclusion holds for $\widetilde{U}$ states [these are the energy eigenfunctions $|\psi_{\boldsymbol{k}}, J, t', t''\rangle$ when $J < J_c(\boldsymbol{k}, t', t'')$].

In order to complement the above real space picture, one also considers the hole momentum distribution function

$$n^{Y}_{\boldsymbol{k}}(\boldsymbol{q}, \sigma) \equiv \langle Y_{\boldsymbol{k}} | \widetilde{c}_{-\boldsymbol{q}, -\sigma} \widetilde{c}^{\dagger}_{-\boldsymbol{q}, -\sigma} | Y_{\boldsymbol{k}} \rangle \qquad (4)$$

for $Y = Q, U$. Since Q states bear an electron-like character, the hole momentum distribution function $n^{Q}_{\boldsymbol{k}}(\boldsymbol{q}, +1/2)$ is peaked at $\boldsymbol{q} = \boldsymbol{k}$. A smaller peak is also observed at $\boldsymbol{q} = \boldsymbol{k} + (\pi, \pi)$ due to the strong AF correlations [45]. In U states, the hole strongly interacts with the surrounding spins and, as a result, the hole momentum distribution function $n^{U}_{\boldsymbol{k}}(\boldsymbol{q}, +1/2)$ peaks around $\boldsymbol{q} = (\pi, \pi)$ for all momenta $\boldsymbol{k}$ (Fig. 3a). Table 2 illustrates that the hole density in $\widetilde{U}$ states also peaks around (π, π) independently of the momentum $\boldsymbol{k}$.

The above results confirm that Q states capture the AF correlations that persist around the vacancy away from half-filling. This is expected since these states have a well defined quasiparticle character. A remarkably different picture holds for the U and $\widetilde{U}$ states, whose quasiparticle spectral weight vanishes. As the above spin density results indicate, the spin correlations in these states spread the extra $S^z = 1/2$ away from the vacancy. The resulting loss of spin exchange energy is accompanied by a gain in the hole kinetic energy, as it follows from the hole momentum distribution results which support that, in these states, the hole always lies around the bare band bottom [which is located at (π, π)]. This evidence resembles predictions from spin-charge separation scenarios. Indeed, within the slave-boson [7,46,47] and doped-carrier frameworks [10,36], the electron decays into a charged spinless boson, which condenses at (π, π), and a spin-1/2 chargeless fermion, which carries the remaining momentum. The above calculations determine the equal time correlations probed by the quantities in equations (3) and (4) in a small lattice and, thus, cannot prove the existence (or lack thereof) of true spin-charge separation. Still, they support that, in U and $\widetilde{U}$ states, the lattice spins screen the hole in conformity with short-range aspects of spin-charge separation phenomenology.

3.2 Effect on electron dynamics

The different hopping terms in the $tt't''J$ model Hamiltonian (Eq. (1)) move electrons between first, second and third NN sites under the no-double-occupancy constraint. These processes may or may not be restrained by the surrounding spin correlations [48]. For instance, NN hopping is frustrated by the two-sublattice structure

Table 2. $\sum'_{\boldsymbol{q}} n^{\widetilde{U}}_{\boldsymbol{k}}(\boldsymbol{q},+1/2) \equiv \sum'_{\boldsymbol{q}} \langle \widetilde{U}_{\boldsymbol{k}}|\widetilde{c}_{-\boldsymbol{q},-1/2}\widetilde{c}^{\dagger}_{-\boldsymbol{q},-1/2}|\widetilde{U}_{\boldsymbol{k}}\rangle$. $\boldsymbol{q}=(0,0)$ results involve sum over $\boldsymbol{q}=(0,0)$, $\boldsymbol{q}=(\pm\pi/2,0)$ and $\boldsymbol{q}=(0,\pm\pi/2)$. $\boldsymbol{q}=(\pi,\pi)$ results involve sum over $\boldsymbol{q}=(\pi,\pi)$, $\boldsymbol{q}=(\pm\pi/2,\pi)$ and $\boldsymbol{q}=(\pi,\pm\pi/2)$. The model parameters used are relevant to both hole doped cuprates ($J=0.4$, $t'=-0.3$, $t''=0.2$) and electron doped cuprates ($J=0.4$, $t'=0.3$, $t''=-0.2$) [44].

	$t'=-0.3; t''=0.2$		$t'=0.3; t''=-0.2$	
$\boldsymbol{k}$	$(\pi,0)$	$(0,0)$	$(\frac{\pi}{2},\frac{\pi}{2})$	$(0,0)$
$\boldsymbol{q}=(0,0)$	0.0329	0.0343	0.0164	0.0328
$\boldsymbol{q}=(\pi,\pi)$	0.5437	0.6051	0.5293	0.5141

Table 3. ΔE^{Q}, ΔE^{U}, ΔE^{ψ} and $W^{Q}_{\boldsymbol{k}}$ with $\boldsymbol{k}=\boldsymbol{k'}\equiv(\pi,0)$ and $\boldsymbol{k}=\boldsymbol{k''}\equiv(\pi/2,\pi/2)$ for several t' and t'' and $J=0.4$.

t'	t''	ΔE^{ψ}	ΔE^{Q}	ΔE^{U}	$W^{Q}_{\boldsymbol{k'}}$	$W^{Q}_{\boldsymbol{k''}}$
–0.3	0.2	0.69	1.43	0.22	0	0.75
–0.2	0.1	0.56	0.92	0.14	0.45	0.72
0	0	0	0	0	0.66	0.66
0.2	–0.1	–0.75	–1.08	–0.10	0.76	0.50
0.3	–0.2	–0.80	–2.33	–0.29	0.82	0

of AF correlations. Intra-sublattice hopping processes are, however, consistent with the staggered pattern of AF correlations which, thus, do not strongly renormalize t' and t'' [49].

The way the spin correlations in U states renormalize t, t' and t'' is strikingly different though. Firstly, these correlations are induced as a way to enhance NN hopping. Secondly, they heavily renormalize t' and t''. To establish the latter fact, consider the hole dispersion in Q states $E^{Q}_{\boldsymbol{k}} \equiv \langle Q_{\boldsymbol{k}}|H_{tt't''J}|Q_{\boldsymbol{k}}\rangle$ and the hole dispersion in U states $E^{U}_{\boldsymbol{k}} \equiv \langle U_{\boldsymbol{k}}|H_{tt't''J}|U_{\boldsymbol{k}}\rangle$. Table 3 displays how the dispersion width between $(\pi,0)$ and $(\pi/2,\pi/2)$ changes with t' and t'' for both Q states ($\Delta E^{Q} \equiv E^{Q}_{(\pi,0)} - E^{Q}_{(\pi/2,\pi/2)}$) and U states ($\Delta E^{U} \equiv E^{U}_{(\pi,0)} - E^{U}_{(\pi/2,\pi/2)}$) [50]. Indeed, the effect of t' and t'' on ΔE^{Q} is almost one order of magnitude larger than on ΔE^{U}.

Interestingly, certain spin liquid correlations discussed in the context of the tJ model strongly inhibit coherent intra-sublattice hopping [51]. This fact, together with the above results, further supports that spin correlations in U states resemble spin liquid correlations at short length scales.

4 Momentum space anisotropy

In the cuprates' renowned pseudogap metallic regime, the low energy physics is determined by the states around the $(\pi,0)-(0,\pi)$ line [21]. However, there is a clear distinction between the nodal [$\boldsymbol{k}=(\pm\pi/2,\pm\pi/2)$] and the antinodal [$\boldsymbol{k}=(\pi,0)$, $(0,\pi)$] regions. Specifically, ARPES detects an energy difference between the single-electron spectral features around $(\pi/2,\pi/2)$ and $(\pi,0)$ (whence the term "pseudogap") [21,52] and, in addition, a strong suppression of the electronic character of excitations is observed in the pseudogap region. These phenomena occur in both hole and electron doped compounds with a crucial difference: in the former, low energy quasiparticles appear close to $(\pi/2,\pi/2)$ but not around $(\pi,0)$ [18,19,24,27]; in electron doped materials, both the pseudogap and the excitations with little electron-like character are pushed toward the zone diagonal [25,53,54].

This phenomenology is reproduced by the generalized-tJ model, due to the role of the intra-sublattice hopping parameters t' and t''. Indeed, for $t',t''=0$, the quasiparticle states at $(\pi/2,\pi/2)$ and $(\pi,0)$ have both comparable energies and spectral weight intensities [32,55]. On the other hand, non-zero t' and t'' fit the experimentally observed dispersion width along $(\pi,0)-(\pi/2,\pi/2)$ [9,28,56,57]. These intra-sublattice hopping parameters further lead to pseudogap states with modified spin background correlations [8,58,59] and, thus, with small spectral weight [9,10,14,17,28,44]. As to the difference between the hole and electron doped regimes, it simply follows from the change in the sign of t' and t'' [9,10,14,17,28,29,56].

The main message of this paper is that the results obtained in Sections 2 and 3 provide a microscopic two-band picture that rationalizes the above generalized-tJ model behavior. This picture embodies the effect of the Q and U states' short-range correlations, which underlies the momentum anisotropic pseudogap behavior, as well as its dependence on electronic density (see below).

4.1 Two-band picture

Section 2.2 identifies the two distinct spin correlations that dress the vacancy in low energy single-hole states. The static properties of these low energy states then follow from the reduced two-band Hamiltonian [40]

$$H_{reduced,\boldsymbol{k}} \equiv \begin{bmatrix} \langle Q_{\boldsymbol{k}}|H_{tt't''J}|Q_{\boldsymbol{k}}\rangle & \langle Q_{\boldsymbol{k}}|H_{tt't''J}|U_{\boldsymbol{k}}\rangle \\ \langle U_{\boldsymbol{k}}|H_{tt't''J}|Q_{\boldsymbol{k}}\rangle & \langle U_{\boldsymbol{k}}|H_{tt't''J}|U_{\boldsymbol{k}}\rangle \end{bmatrix}. \quad (5)$$

This Hamiltonian yields the two spectral dispersions observed both by ARPES data [18–20,22] and by various theoretical studies of the related tJ and Hubbard models [10–14,16]. It also determines the hybridization of Q and U states and, thus, the spectral weight distribution throughout momentum space. Therefore, $H_{reduced,\boldsymbol{k}}$ must capture the aforementioned role of t' and t'' in the pseudogap phenomenology.

Interestingly, the above role of t' and t'' can be discussed only in terms of the dispersions $E^{Q}_{\boldsymbol{k}}$ and $E^{U}_{\boldsymbol{k}}$. To see this, note that t' and t'' strongly affect the dispersion of a hole surrounded by the AF correlations in Q states [in fact, $\Delta E^{Q} = A(-4t'+8t'')$, where the renormalization factor $A \gtrsim 1/2$]. Therefore, $t'<0$ and $t''>0$ increase the energy $E^{Q}_{(\pi,0)}$ and decrease $E^{Q}_{(\pi/2,\pi/2)}$. Consequently, $E^{\psi}_{(\pi,0)} \equiv \langle \psi_{(\pi,0)}|H_{tt't''J}|\psi_{(\pi,0)}\rangle$ also increases and $E^{\psi}_{(\pi/2,\pi/2)} \equiv \langle \psi_{(\pi/2,\pi/2)}|H_{tt't''J}|\psi_{(\pi/2,\pi/2)}\rangle$ also decreases and, hence, a pseudogap $\Delta E^{\psi} \equiv E^{\psi}_{(\pi,0)} - E^{\psi}_{(\pi/2,\pi/2)}$ opens at $(\pi,0)$. Intra-sublattice hopping is, however, strongly

frustrated in U states and, thus, $t' < 0$ and $t'' > 0$ increase the energy difference $E^Q_{(\pi,0)} - E^U_{(\pi,0)}$ while reducing $E^Q_{(\pi/2,\pi/2)} - E^U_{(\pi/2,\pi/2)}$ (Figs. 3b, 3c). This impacts the extent to which $|Q_{\boldsymbol{k}}\rangle$ and $|U_{\boldsymbol{k}}\rangle$ hybridize, reducing $W^Q_{(\pi,0)} \equiv |\langle\psi_{(\pi,0)}|Q_{(\pi,0)}\rangle|^2$ while enlarging $W^Q_{(\pi/2,\pi/2)} \equiv |\langle\psi_{(\pi/2,\pi/2)}|Q_{(\pi/2,\pi/2)}\rangle|^2$ (Tab. 3). For $J = 0.4$, $t' = -0.3$, $t'' = 0.2$ the energy $E^Q_{(\pi,0)}$ is so large that the minimum energy obtained by a linear combination of $|Q_{(\pi,0)}\rangle$ and $|U_{(\pi,0)}\rangle$ becomes higher than that of a different state $|\widetilde{U}_{(\pi,0)}\rangle$ with vanishing quasiparticle spectral weight (Fig. 3b). As a result, $W^Q_{(\pi,0)} = 0$. Since, at the same time, $W^Q_{(\pi/2,\pi/2)} = 0.75$, nodal and antinodal states display a sharply different electron-like character [8,58,59].

The change between the cuprates' hole and electron doped regimes amounts to a change in the sign of t' and t'', in which case $\Delta E^Q = A(-4t' + 8t'')$ changes sign as well. The above argument then still applies, with the roles of momenta $(\pi, 0)$ and $(\pi/2, \pi/2)$ interchanged (Fig. 3d and Tab. 3).

4.2 Doping dependence

The above calculation and the ensuing arguments concern a single hole surrounded by a spin background and, thus, do not have to straightforwardly apply in the presence of a finite hole density. Interestingly, though, a large body of evidence suggests that single-hole physics is relevant away from half-filling. Indeed, quantum Monte Carlo [11,12], exact diagonalization [13] and cellular dynamical mean-field theory [14] studies show that the two-band structure identified in the half-filled spectral function below the chemical potential remains almost unaffected upon hole doping, whose main effect is to transfer spectral weight between the pre-existing bands in a momentum dependent manner. This behavior is expected as long as short-range AF correlations are present [11–13]. Since calculations on the $U/t = 8$ Hubbard model [60] find that such correlations persist around the vacancy up to the hole density $x = 0.25$, the above two-band picture may apply in a wide doping range. Cuprate ARPES data also displays the two dispersive features throughout a large portion of the phase diagram [18–22], hence, it complies with the aforementioned theoretical expectations.

It is well-known that the pseudogap phenomenology weakens upon increasing the dopant density. Hence, the pseudogap magnitude diminishes away from half-filling [21,26], as does the difference in the electron-like character of nodal and antinodal excitations [18,19,24,25,27]. This experimental evidence is captured by the naive extension of the above two-band picture to the finite hole density case. Indeed, Section 4.1 shows that the momentum space anisotropic behavior follows from the effect of t' and t'' in the dynamics of holes surrounded by short-range AF correlations. Upon doping, these correlations are gradually replaced by the doping induced correlations which prevail in U states. Since the latter strongly renormalize t' and t'', the differentiation between the $(\pi/2, \pi/2)$ and $(\pi, 0)$ regions is also gradually depleted.

References [10,36] develop a new mean-field approach to the $tt't''J$ model that embodies the above two-band picture in the presence of a finite hole density. It explicitly captures the interplay between the mobile holes and the above two different spin correlations and correctly describes the microscopic electron dynamics in the 2D doped Mott insulator. This assertion is attested by the successful comparison to other theoretical approaches and especially to a vast portfolio of non-trivial cuprate ARPES and tunneling conductance data. The latter include the aforementioned nodal-antinodal dichotomy, the Fermi arcs, the peak-dip-hump structure, the kink and the extended flat regions close to $(\pi, 0)$ in the electron dispersion and the large diversity of tunneling spectra [10,61].

5 Conclusions

In this paper, I numerically study how a single mobile hole is dressed by the encircling spins within the $tt't''J$ model context. Purely local energetic arguments decide whether a staggered moment configuration or a spin configuration reminiscent of spin liquid physics prevails around the vacancy. In the experimentally relevant parameter regime, the competition between the two spin correlations is very subtle and can be particularly sensitive to the hole momentum. Consequently, the electron spectral properties can be extremely momentum dependent, displaying a pseudogap and distinct quasiparticle properties in the nodal and antinodal regions, as observed in both hole and electron doped cuprate compounds [18,19,21,24–28]. AF short-range correlations are gradually depleted upon doping and, thus, the above differentiation between the nodal and antinodal regions is expected to disappear further away from half-filling, in agreement with the phenomenology of high-T_c superconductors [21,24–27].

The above considerations agree with prior work [11,14,61–64] substantiating that the pseudogap and the resulting momentum space anisotropy follow from the local interaction between the doped carriers and the short-range spin correlations that strive close to the Mott insulating transition. This paper goes a step further and provides a scheme to determine the local spin correlations that dress moving carriers. In particular, it shows that the interplay between the itinerant doped carrier and the surrounding local moments translates into the coexistence of two different local correlations, namely the staggered moment correlations already present in the undoped system and a different type of correlations induced upon carrier doping. The latter correlations are shown to be responsible for short-range phenomenology characteristic of spin-charge separated states and to have a peculiar impact in the electron dynamics, specifically, they strongly renormalize t' and t''.

One way to optimize both the hole kinetic energy and the spin exchange energy in doped Mott insulators is to spatially separate charge and spin degrees of freedom into, say, static stripe-like configurations [65]. The above calculation suggests an alternative scenario: the quantum

superposition of two types of local states which separately enhance the J and t terms of the Hamiltonian. These two states have a drastically different effect on the electron dynamics and provide a simple two-band microscopic picture of doped Mott insulators. In this picture, the vacancy is, at times, surrounded by staggered moments while, at other instants, spin liquid correlations take over in order to facilitate the vacancy's motion. In the pseudogap momentum space region, the kinetic energy of a vacancy surrounded by a local AF spin configuration increases with $|t'|$ and $|t''|$, thus tilting the balance in favor of the above spin liquid correlations (whose energy is less sensitive to t' and t''). As a result, in the pseudogap regime, the way the spin background dresses the hole at $(\pi/2, \pi/2)$ differs from the way it dresses the hole at $(\pi, 0)$. This fact is in consonance with previous numerical evidence for the approximate decoupling of spin and charge degrees of freedom in the pseudogap states [8,58,59].

Finally, I remark that the above two-band picture provides the basis to develop new approximate schemes to describe doped Mott insulators. The mean-field theory developed in references [10,36] constitutes one such example. Remarkably, this approach reproduces a variety of experimental data [10,61].

This work was partially supported by the Fundação Calouste Gulbenkian Grant No. 58119 (Portugal), NSF Grant No. DMR-01-23156, NSF-MRSEC Grant No. DMR-02-13282 and by the DOE Grant No. DE-AC02-05CH11231.

References

1. N.F. Mott, Proc. Phys. Soc. (London) A **62**, 416 (1949)
2. P.W. Anderson, Phys. Rev. **115**, 2 (1959)
3. J. Hubbard, Proc. Roy. Soc. (London) A **276**, 238 (1963)
4. M. Imada, A. Fujimori, Y. Tokura, Rev. Mod. Phys. **70**, 1039 (1998)
5. P.W. Anderson, Science **235**, 1196 (1987)
6. E. Dagotto, Rev. Mod. Phys. **66**, 763 (1994)
7. P.A. Lee, N. Nagaosa, X.-G. Wen, Rev. Mod. Phys. **78**, 17 (2006)
8. T. Tohyama, Y. Shibata, S. Maekawa, Z.-X. Shen, N. Nagaosa, L.L. Miller, J. Phys. Soc. Jpn **69**, 9 (2000)
9. T. Tohyama, Phys. Rev. B **70**, 174517 (2004)
10. T.C. Ribeiro, X.-G. Wen, Phys. Rev. Lett. **95**, 057001 (2005a)
11. R. Preuss, W. Hanke, W. von der Linden, Phys. Rev. Lett. **75**, 1344 (1995)
12. C. Gröber, R. Eder, W. Hanke, Phys. Rev. B **62**, 4336 (2000)
13. A. Moreo, S. Haas, A.W. Sandvik, E. Dagotto, Phys. Rev. B **51**, R12045 (1995)
14. B. Kyung, S.S. Kancharla, D. Sénéchal, A.-M.S. Tremblay, M. Civelli, G. Kotliar, Phys. Rev. B **73**, 165114 (2006a)
15. O. Parcollet, G. Biroli, G. Kotliar, Phys. Rev. Lett. **92**, 226402 (2004)
16. A. Dorneich, M.G. Zacher, C. Gröber, R. Eder, Phys. Rev. B **61**, 12816 (2000)
17. M. Civelli, M. Capone, S.S. Kancharla, O. Parcollet, G. Kotliar, Phys. Rev. Lett. **95**, 106402 (2005)
18. T. Yoshida, X.J. Zhou, T. Sasagawa, W.L. Yang, P.V. Bogdanov, A. Lanzara, Z. Hussain, T. Mizokawa, A. Fujimori, H. Eisaki et al., Phys. Rev. Lett. **91**, 027001 (2003)
19. F. Ronning, T. Sasagawa, Y. Kohsaka, K.M. Shen, A. Damascelli, C. Kim, T. Yoshida, N.P. Armitage, D.H. Lu, D.L. Feng et al., Phys. Rev. B **67**, 165101 (2003)
20. Y. Kohsaka, T. Sasagawa, F. Ronning, T. Yoshida, C. Kim, T. Hanaguri, M. Azuma, M. Takano, Z.-X. Shen, H. Takagi, J. Phys. Soc. Jpn **72**, 1018 (2003)
21. A. Damascelli, Z.-X. Shen, Z. Hussain, Rev. Mod. Phys. **75**, 473 (2003)
22. K.M. Shen, F. Ronning, D.H. Lu, W.S. Lee, N.J.C. Ingle, W. Meevasana, F. Baumberger, A. Damascelli, N.P. Armitage, L.L. Miller et al., Phys. Rev. Lett. **93**, 267002 (2004)
23. This statement finds support in various theoretical and experimental results. For instance: (i) analytical methods show that AF correlations suppress *inter*-sublattice hopping [32–34,66] while certain spin liquid correlations suppress *intra*-sublattice processes instead [51]; (ii) exact diagonalization [13], quantum Monte Carlo [11], cluster perturbation theory [62] and cellular dynamical mean-field theory [14,64] show how electronic spectral features keep track of the underlying local correlations; (iii) the ubiquitous flat bands observed in the cuprates around $(\pi, 0)$ [67] follow from the local spin correlations as well [55,61]; (iv) AF correlations renormalize the cuprate nodal dispersion width down to $\approx 2.2J$ [6,8,19–22,28,26]
24. X.J. Zhou, T. Yoshida, D.-H. Lee, W.L. Yang, V. Brouet, F. Zhou, W.X. Ti, J.W. Xiong, Z.X. Zhao, T. Sasagawa et al., Phys. Rev. Lett. **92**, 187001 (2004)
25. N.P. Armitage, F. Ronning, D.H. Lu, C. Kim, A. Damascelli, K.M. Shen, D.L. Feng, H. Eisaki, Z.-X. Shen, P.K. Mang et al., Phys. Rev. Lett. **88**, 257001 (2002)
26. K. Tanaka, T. Yoshida, A. Fujimori, D.H. Lu, Z.-X. Shen, X.-J. Zhou, H. Eisaki, Z. Hussain, S. Uchida, Y. Aiura et al., Phys. Rev. B **70**, 092503 (2004)
27. A. Kaminski, H.M. Fretwell, M.R. Norman, M. Randeria, S. Rosenkranz, U. Chatterjee, J.C. Campuzano, J. Mesot, T. Sato, T. Takahashi et al., Phys. Rev. B **71**, 014517 (2005)
28. C. Kim, P.J. White, Z.-X. Shen, T. Tohyama, Y. Shibata, S. Maekawa, B.O. Wells, Y.J. Kim, R.J. Birgeneau, M.A. Kastner, Phys. Rev. Lett. **80**, 4245 (1998)
29. T. Tohyama, S. Maekawa, Phys. Rev. B **49**, 3596 (1994)
30. Y. Nagaoka, Phys. Rev. **147**, 392 (1966)
31. S.R. White, I. Affleck, Phys. Rev. B **64**, 024411 (2001)
32. G. Martinez, P. Horsch, Phys. Rev. B **44**, 317 (1991)
33. S. Schmitt-Rink, C.M. Varma, A.E. Ruckenstein, Phys. Rev. Lett. **60**, 2793 (1988)
34. A. Ramšak, P. Horsch, Phys. Rev. B **57**, 4308 (1998)
35. K.G. Wilson, Rev. Mod. Phys. **47**, 773 (1975)
36. T.C. Ribeiro, X.-G. Wen, Phys. Rev. B **74**, 155113 (2006)
37. Note the difference between the kets $|\widetilde{U}_{\boldsymbol{k}}, J, t', t''\rangle$ and $|U_{\boldsymbol{k}}, t', t''\rangle$. The former is *J-dependent* and is defined for $J < J_c(\boldsymbol{k}, t', t'')$. The latter is *J-independent* and is defined for $J > J_c(\boldsymbol{k}, t', t'')$. Similar notation is used for both states since they have similar properties in the parameter regime of interest to the cuprates (see Sect. 3).
38. The above choice of $J = 0.2$ and $J = 0.6$ could have been made different. However, any reasonable set of two values of J in the range $[0.2, 0.8]$ would lead to similar conclusions

39. The width of the interval of J values displayed in Table 1, namely $[0.2, 0.8]$, is of the order of the maximum J value.
40. As it follows from the approximate equality in equation (2), the states $|Q_{\boldsymbol{k}}, t', t''\rangle$ and $|U_{\boldsymbol{k}}, t', t''\rangle$ are relatively insensitive to variations of the two values of J used to define the above mentioned 2D plane in the single hole $tt't''J$ model Hilbert space. In the limit where these two values of J become infinitesimally close to each other, $|Q_{\boldsymbol{k}}, t', t''\rangle$ and $|U_{\boldsymbol{k}}, t', t''\rangle$ are constructed from the state vectors $|\psi_{\boldsymbol{k}}, J, t', t''\rangle$ and $\partial|\psi_{\boldsymbol{k}}, J, t', t''\rangle/\partial J$. Therefore, one can determine a pair of Q and U states for every single value of $J > J_c(\boldsymbol{k}, t', t'')$
41. This is the region where the lowest eigenstates lie and whose properties one is more concerned about
42. The above formal construction to derive Q and U states can be applied, for instance, to the 3D $tt't''J$ model. However, in that case, U states are expected to be less relevant since AF correlations, which are more robust in 3D, lead to strong quasiparticle properties throughout the Brillouin zone
43. The average magnetization $\frac{1}{N-1}\sum_j \langle S_j^z\rangle = \frac{1}{N-1}\frac{1}{2}$, where N is the number of lattice sites, is subtracted to reduce finite size effects
44. T. Tohyama, S. Maekawa, Supercond. Sci. Technol. **13**, R17 (2000)
45. R. Eder, Y. Ohta, Phys. Rev. B **51**, 6041 (1995)
46. P.A. Lee, N. Nagaosa, Phys. Rev. B **46**, 5621 (1992)
47. X.-G. Wen, P.A. Lee, Phys. Rev. Lett. **76**, 503 (1996)
48. This is the reason why electronic spectral properties provide an indirect probe of the local correlations [23]
49. As shown in reference [8], the hole dispersion in the $tt't''J$ model along $(0,\pi)-(\pi,0)$ is controlled by $t' \approx -2t''$ and is a factor $\sim$2–3 smaller than expected from the bare parameters. This is to be contrasted with the nodal dispersion width which goes from the bare value $8t$ down to $2.2J$ due to AF spin correlations [6,8,21,32,66]. In the parameter regime of interest to the cuprates this corresponds to a renormalization by a factor of $\sim$10
50. The fact that this width vanishes for $t', t'' = 0$ is an artifact of the 4×4 lattice [68]. In larger systems, the dispersion width along $(\pi, 0) - (\pi/2, \pi/2)$ for $t', t'' = 0$ is $\approx$20% of the nodal dispersion width [32,55]
51. T.C. Ribeiro, X.-G. Wen, Phys. Rev. B **68**, 024501 (2003)
52. H. Ding, T. Yokoya, J.C. Campuzano, T. Takahashi, M. Randeria, M.R. Norman, T. Mochiku, K. Kadowaki, J. Giapintzakis, Nature **382**, 51 (1996)
53. A. Koitzsch, G. Blumberg, A. Gozar, B.S. Dennis, P. Fournier, R.L. Greene, Phys. Rev. B **67**, 184522 (2003)
54. R.W. Hill, C. Proust, L. Taillefer, P. Fournier, R.L. Greene, Nature **414**, 711 (2001)
55. E. Dagotto, A. Nazarenko, M. Boninsegni, Phys. Rev. Lett. **73**, 728 (1994)
56. R.J. Gooding, K.J.E. Vos, P.W. Leung, Phys. Rev. B **50**, 12866 (1994)
57. A. Nazarenko, K.J.E. Vos, S. Haas, E. Dagotto, R.J. Gooding, Phys. Rev. B **51**, 8676 (1995)
58. W.-C. Lee, T.K. Lee, C.-M. Ho, P.W. Leung, Phys. Rev. Lett. **91**, 057001 (2003)
59. G.B. Martins, R. Eder, E. Dagotto, Phys. Rev. B **60**, R3716 (1999)
60. D. Duffy, A. Moreo, Phys. Rev. B **51**, 11882 (1995)
61. T.C. Ribeiro, X.-G. Wen, Phys. Rev. Lett. **97**, 057003 (2006)
62. D. Sénéchal, A.M.S. Tremblay, Phys. Rev. Lett. **92**, 126401 (2004)
63. T.D. Stanescu, P. Phillips, Phys. Rev. Lett. **91**, 017002 (2003)
64. B. Kyung, G. Kotliar, A.-M.S. Tremblay, Phys. Rev. B **73**, 205106 (2006b)
65. J. Zaanen, O. Gunnarsson, Phys. Rev. B **40**, 7391 (1989)
66. C.L. Kane, P.A. Lee, N. Read, Phys. Rev. B **39**, 6880 (1989)
67. D.M. King, Z.-X. Shen, D.S. Dessau, D.S. Marshall, C.H. Park, W.E. Spicer, J.L. Peng, Z.Y. Li, R.L. Greene, Phys. Rev. Lett. **73**, 3298 (1994)
68. E. Dagotto, R. Joynt, A. Moreo, S. Bacci, E. Gagliano, Phys. Rev. B **41**, 9049 (1990)